

See discussions, stats, and author profiles for this publication at: <https://www.researchgate.net/publication/6627489>

Synthesis, crystal structure, and luminescent properties of novel Eu 3+ heterocyclic β -diketonate complexes with bidentate nitrogen donors

ARTICLE in INORGANIC CHEMISTRY · JANUARY 2007

Impact Factor: 4.76 · DOI: 10.1021/ic061425a · Source: PubMed

CITATIONS

136

READS

81

4 AUTHORS, INCLUDING:



Biju Silvanose

University of Leuven

29 PUBLICATIONS 942 CITATIONS

SEE PROFILE



MLP Reddy

National Institute for Interdisciplinary Scienc...

119 PUBLICATIONS 2,399 CITATIONS

SEE PROFILE



Benson Kariuki

Cardiff University

348 PUBLICATIONS 5,032 CITATIONS

SEE PROFILE

Synthesis, Crystal Structure, and Luminescent Properties of Novel Eu^{3+} Heterocyclic β -Diketonate Complexes with Bidentate Nitrogen Donors

S. Biju,[†] D. B. Ambili Raj,[†] M. L. P. Reddy,^{*,†} and B. M. Kariuki[‡]

Chemical Science and Technology Division, Regional Research Laboratory, CSIR, Thiruvananthapuram 695 019, India, and School of Chemical Sciences, University of Birmingham, Birmingham, U.K. B15 2TT

Received July 29, 2006

New tris(heterocyclic β -diketonato)europium(III) complexes of the general formula $\text{Eu}(\text{PBI})_3 \cdot \text{L}$ [where HPBI = 3-phenyl-4-benzoyl-5-isoxazalone and $\text{L} = \text{H}_2\text{O}$, 2,2'-bipyridine (bpy), 4,4'-dimethoxy-2,2'-bipyridine (dmbpy), 1,10-phenanthroline (phen), or 4,7-diphenyl-1,10-phenanthroline (bath)] were synthesized and characterized by elemental analysis, Fourier transform infrared spectroscopy (FT-IR), ^1H NMR, high-resolution mass spectrometry, thermogravimetric analysis, and photoluminescence (PL) spectroscopy. Single-crystal X-ray structures have been determined for the complexes $\text{Eu}(\text{PBI})_3 \cdot \text{H}_2\text{O} \cdot \text{EtOH}$ and $\text{Eu}(\text{PBI})_3 \cdot \text{phen}$. The complex $\text{Eu}(\text{PBI})_3 \cdot \text{H}_2\text{O} \cdot \text{EtOH}$ is mononuclear, and the central Eu^{3+} ion is coordinated by eight oxygen atoms to form a bicapped trigonal prism coordination polyhedron. Six oxygens are from the three bidentate HPBI ligands, one is from a water molecule, and another is from an ethanol molecule. On the other hand, the crystal structure of $\text{Eu}(\text{PBI})_3 \cdot \text{phen}$ reveals a distorted square antiprismatic geometry around the europium atom. The room-temperature PL spectra of the europium(III) complexes are composed of the typical Eu^{3+} red emission, assigned to transitions between the first excited state ($^5\text{D}_0$) and the multiplet ($^7\text{F}_{0-4}$). The results demonstrate that the substitution of solvent molecules by bidentate nitrogen ligands in $\text{Eu}(\text{PBI})_3 \cdot \text{H}_2\text{O} \cdot \text{EtOH}$ richly enhances the quantum yield and lifetime values. To elucidate the energy transfer process of the europium complexes, the energy levels of the relevant electronic states have been estimated. Judd–Ofelt intensity parameters (Ω_2 and Ω_4) were determined from the emission spectra for Eu^{3+} ion based on the $^5\text{D}_0 \rightarrow ^7\text{F}_2$ and $^5\text{D}_0 \rightarrow ^7\text{F}_4$ electronic transitions, respectively, and the $^5\text{D}_0 \rightarrow ^7\text{F}_1$ magnetic dipole allowed transition was taken as the reference. The high values obtained for the 4f–4f intensity parameter Ω_2 for europium complexes suggest that the dynamic coupling mechanism is quite operative in these compounds.

Introduction

Lanthanide complexes with organic ligands are of great interest for a wide range of photonic applications such as tunable lasers, amplifiers for optical communications, components of the emitting materials in multilayer organic light-emitting diodes, and efficient light conversion molecular devices.^{1–5} In most cases, the luminescent complexes consist

of a central lanthanide ion and chelating organic ligand as a photosensitizer. The antenna chromophore moiety efficiently absorbs and transfers light to the central lanthanide ion by the energy transfer process. This sensitization process is much more effective than the direct excitation of the Ln^{3+} ions, since the absorption coefficients of organic chromophores are many orders of magnitude larger than the intrinsically low molar absorption coefficients (typically $1\text{--}10\text{ M}^{-1}\text{ cm}^{-1}$) of lanthanide ions.⁶

The β -diketone ligand is one of the important “antennas”, from which the energy can be effectively transferred to Ln^{3+} ions for high harvest emissions and which has the following

* To whom correspondence should be addressed. Telephone: 91-471-2515360. Fax: 91-471-2491712. E-mail: mlpreddy@yahoo.co.uk.

[†] CSIR.

[‡] University of Birmingham.

- (1) Bunzli, J. C. G.; Piguet, C. *Chem. Soc. Rev.* **2005**, *34*, 1048–1077.
- (2) Bunzli, J. C. G.; Piguet, C. *Chem. Rev.* **2002**, *102*, 1897–1928.
- (3) Kido, J.; Okamoto, Y. *Chem. Rev.* **2002**, *102*, 2357–2368.
- (4) Reyes, R.; Cremona, M.; Teotonio, E. E. S.; Brito, H. F.; Malta, O. L. *Thin Solid Films* **2004**, *196*, 165–195.
- (5) de Sa, G. F.; Malta, O. L.; de Mello Donega, C.; Simas, A. M.; Longo, R. L.; Santa-Cruz, P. A.; da Silva, E. F., Jr. *Coord. Chem. Rev.* **2000**, *196*, 165–195.

- (6) (a) Carnall, W. T.; Gruen, D. M.; McBeth, R. L. *J. Phys. Chem.* **1962**, *66*, 2159. (b) Carnall, W. T. *J. Phys. Chem.* **1963**, *67*, 1206. (c) Carnall, W. T.; Fields, P. R.; Wybourne, B. G. *J. Chem. Phys.* **1965**, *42*, 3797. (d) Kim, Y. H.; Baek, N. S.; Kim, H. K. *ChemPhysChem* **2006**, *7*, 213–221.

advantages.⁵ The β -diketone ligand has strong absorption within a large wavelength range for its π – π^* transition and consequently has been targeted for its ability to sensitize the luminescence of the Ln^{3+} ions. Further, it has the ability to form stable and strong adducts with Ln^{3+} ions, which can have practical usage.^{7,8} A large number of highly coordinated complexes of lanthanide tris(β -diketonates) containing several nitrogen ligands such as 1,10-phenanthroline,⁹ 4,7-disubstituted-1,10-phenanthrolines,¹⁰ 2,2'-bipyridine,¹⁰ 4,4'-disubstituted-2,2'-bipyridines,¹⁰ 1,4-diaza-1,3-butadienes,¹¹ and 2,2':6',6''-terpyridine^{12,13} have been reported as efficient light conversion molecular devices. Highly efficient photoluminescent and electroluminescent performances have also been observed in the europium(III)–(tris-2-thenoyltrifluoroacetate)phosphine oxide complexes.¹⁴ Molecular lanthanide chelates containing 4-acyl-5-pyrazolonate ligands have also been successfully used in the production of emission layers in organic electroluminescent devices.^{15,16} Recently, the authors have developed promising light conversion molecular devices based on 3-phenyl-4-aryloyl-5-isoxazolonate complexes of Eu^{3+} with phosphine oxides, which provides stable eight- and nine-coordinated lanthanide complexes with high quantum efficiency.^{17,18} In the present paper we report the synthesis, crystal structures, and photophysical properties of new europium(III) complexes of 3-phenyl-4-benzoyl-5-isoxazolone (HPBI) with various bidentate nitrogen ligands having electron-donating and electron-withdrawing groups.

Experimental Section

Materials and Instrumentation. The following commercially available chemicals were used without further purification: europium(III) nitrate hexahydrate, 99.9% (Acros Organics); gadolinium(III) nitrate hexahydrate, 99.9% (Acros Organics); 1,10-phenanthroline monohydrate (Merck); 2,2'-dipyridyl, 99+% (Aldrich); 4,7-diphenyl-1,10-phenanthroline, 97% (Aldrich); 4-4'-dimethoxy-2,2'-bipyridine, 97% (Aldrich). The ligand HPBI was synthesized in our laboratory as mentioned in our previous publication.¹⁸ All other chemicals used were of analytical reagent grade.

- (7) Yang, L.; Gong, Z.; Nie, D.; Lou, B.; Bian, Z.; Guan, M.; Huang, C.; Lee, H. J.; Baik, W. P. *New J. Chem.* **2006**, *30*, 791–796.
- (8) Binmams, K. *Handbook on the Physics and Chemistry of Rare Earths*; Elsevier: Amsterdam, 2005; Vol. 35, Chapter 225, pp 107–272.
- (9) Watson, W. H.; Williams, R. J.; Stemple, N. R. *J. Inorg. Chem.* **1972**, *34*, 501–508.
- (10) Bellucci, A.; Barberio, G.; Crispini, A.; Ghedini, M.; La Deda, M.; Pucci, D. *Inorg. Chem.* **2005**, *44*, 1818–1825.
- (11) Fernandes, J. A.; Ferreira, R. A. S.; Pillinger, M.; Carlos, L. D.; Goncalves, I. S.; Ribeiro-Claro, P. J. A. *Eur. J. Inorg. Chem.* **2004**, 3913–3919.
- (12) Fukuda, Y.; Nakao, A.; Hiyashi, K. *J. Chem. Soc., Dalton Trans.* **2002**, 527–533.
- (13) Cotton, S. A.; Noy, O. E.; Liesener, F.; Raithby, P. R. *Inorg. Chim. Acta* **2003**, *344*, 37–42.
- (14) Hasegawa, Y.; Yamamuro, M.; Wada, Y.; Kanehisa, N.; Kai, Y.; Yanagida, S. *J. Phys. Chem. A* **2003**, *107*, 1697–1702.
- (15) Xin, H.; Shi, M.; Gao, X. C.; Huang, Y. Y.; Gong, Z. L.; Nie, D. B.; Cao, H.; Bian, Z. Q.; Li, F. Y.; Huang, C. H. *J. Phys. Chem. B* **2004**, *108*, 10796–10800.
- (16) Shi, M.; Li, F.; Yi, T.; Zhang, D.; Hu, H.; Huang, C. *Inorg. Chem.* **2005**, *44*, 8929–8936.
- (17) Pavithran, R.; Reddy, M. L. P.; Alves, S., Jr.; Freire, R. O.; Rocha, G. B.; Lima, P. P. *Eur. J. Inorg. Chem.* **2005**, *20*, 4129–4137.
- (18) Pavithran, R.; Saleesh Kumar, N. S.; Biju, S.; Reddy, M. L. P.; Alves, S., Jr.; Freire, R. O. *Inorg. Chem.* **2006**, *45*, 2184–2192.

Elemental analyses were performed with a Perkin-Elmer Series 2 Elemental Analyser 2400. A Nicolet FT-IR 560 Magna Spectrometer using KBr (neat) was used to obtain IR spectral data, and a Bruker 300 MHz NMR spectrometer was used to obtain ^1H NMR spectra of the compounds in CDCl_3 or acetone- d_6 media. Thermogravimetric analyses were carried out using a TGA-50H (Shimadzu, Japan). Mass spectra were recorded using a JEOL JSM 600 fast atom bombardment (FAB) high-resolution mass spectrometer (HRMS). Diffuse reflectance spectra of the europium complexes and the standard phosphor were recorded on a Shimadzu UV-2450 UV–vis spectrophotometer using BaSO_4 as a reference. Absorbances of the ligands and corresponding europium complexes in CH_3CN solution were measured with a UV–vis spectrophotometer (Shimadzu, UV-2450). Photoluminescence (PL) spectra were recorded using a Spex-Fluorolog DM3000F spectrofluorometer with a double grating 0.22 m Spex 1680 monochromator and a 450 W Xe lamp as the excitation source using the front face mode. The lifetime measurements were carried out at room temperature using a Spex 1934 D phosphorimeter.

The overall quantum yields (Φ_{overall}) were measured at room temperature using the technique for powdered samples described by Bril et al.,¹⁹ through the following expression:

$$\Phi_{\text{overall}} = \left(\frac{1 - r_{\text{st}}}{1 - r_{\text{x}}} \right) \left(\frac{A_{\text{x}}}{A_{\text{st}}} \right) \Phi_{\text{st}} \quad (1)$$

where r_{st} and r_{x} are the diffuse reflectance (with respect to affixed wavelength) of the complexes and of the standard phosphor, respectively, and Φ_{st} is the quantum yield of the standard phosphor. The terms A_{x} and A_{st} represent the areas under the complex and standard emission spectra, respectively. To have absolute intensity values, BaSO_4 was used as a reflecting standard. The standard phosphor used was sodium salicylate (Merck), whose emission spectra are formed by a large broad band peaking around 425 nm, with a constant Φ value (60%) for excitation wavelengths between 220 and 380 nm. Three measurements were carried out for each sample, so that the presented Φ_{overall} value corresponds to the arithmetic mean value. The errors in the quantum yield values associated with this technique were estimated within 10%.¹⁹

X-ray single-crystal data were recorded at room temperature on a Bruker Smart 6000 diffractometer equipped with a CCD detector and a copper tube source. Data were processed using SAINTPLUS (SAINTPLUS, program suite for data processing, Bruker AXS, Inc., Madison, WI). Structures were solved and refined using SHELXL-97.²⁰ The uncoordinating ethanol molecule in $\text{Eu}(\text{PBI})_3 \cdot \text{H}_2\text{O} \cdot \text{EtOH}$ is disordered with an occupancy of one-half. The water protons were not located, and hydroxyl protons were placed in positions calculated for optimum hydrogen bonding. Non-hydrogen atoms were refined anisotropically, and a riding model was used for C–H hydrogen atoms. Table 1 shows crystal data, structure refinement parameters, atomic coordinates, and isotropic displacement parameters. The dichloromethane site has 70% occupancy, and hydrogen atom positions were constrained geometrically during refinement in the complex $\text{Eu}(\text{PBI})_3 \cdot \text{phen}$.

Synthesis of $\text{Eu}(\text{PBI})_3 \cdot \text{C}_2\text{H}_5\text{OH} \cdot \text{H}_2\text{O}$ (1). An ethanolic solution of $\text{Eu}(\text{NO}_3)_3 \cdot 6\text{H}_2\text{O}$ (0.5 mmol) was added to a solution of HPBI (1.5 mmol) in ethanol in the presence of NaOH (1.5 mmol).

- (19) (a) Bril, A.; De Jager-Veenis, A. W. *J. Electrochem. Soc.* **1976**, *123*, 396–398. (b) Mello Donega, C. D.; Junior, S. A.; de Sa, G. F. *Chem. Commun.* **1996**, *11*, 1199–1200. (c) Carlos, L. D.; Mello Donega, C. D.; Albuquerque, R. Q.; Junior, S. A.; Menezes, J. F. S.; Malta, O. L. *Mol. Phys.* **2003**, *101*, 1037–1045.
- (20) Sheldrick, G. M. *SHELXL97. Program package for crystal structure determination*; University of Göttingen: Göttingen, Germany, 1998.

Table 1. Crystal Data, Collection, and Structure Refinement Parameters for Complexes **1** and **4**

parameters	1	4
empirical formula	$\text{C}_{51}\text{H}_{41}\text{EuN}_3\text{O}_{11.50}$	$\text{C}_{60.70}\text{H}_{39.40}\text{Cl}_{1.40}\text{EuN}_5\text{O}_9$
fw	1031.83	1184.36
crystal system	monoclinic	triclinic
space group	$P2_1/a$	$P\bar{1}$
cryst size (mm^3)	$0.20 \times 0.20 \times 0.10$	$0.20 \times 0.20 \times 0.10$
temperature (K)	296(2)	296(2)
a (Å)	15.6795(4)	10.5185(4)
b (Å)	21.3364(7)	16.7762(8)
c (Å)	16.1558(6)	16.8211(7)
α (deg)	90	80.343(3)
β (deg)	118.076(2)	75.786(2)
γ (deg)	90	72.842(3)
V (Å ³)	4768.8(3)	2734.7(2)
Z	4	2
ρ_{calcd} (g cm^{-3})	1.437	1.438
μ (mm^{-1})	9.950	9.348
$F(000)$	2092	1195
$R1 [I > 2\sigma(I)]$	0.0348	0.0473
$wR2 [I > 2\sigma(I)]$	0.0895	0.1049
$R1$ (all data)	0.0473	0.0734
$wR2$ (all data)	0.0965	0.1165
GOF	1.019	1.009

Precipitation took place immediately, and the reaction mixture was stirred for 10 h at room temperature (Scheme 1). The product was filtered, washed with ethanol, with water, and then with ethanol, and dried and stored in a desiccator. The complex was then purified by recrystallization from dichloromethane–ethanol mixture. Elemental analysis (%): Calcd for $\text{C}_{50}\text{H}_{38}\text{EuN}_3\text{O}_{11}$ (1007.965): C, 59.58; H, 3.8; N, 4.17. Found: C, 59.75; H, 4.01; N, 4.21. IR (KBr) ν_{max} : 3300, 1641, 1614, 1483, 1389, 1184, 910, 760 cm^{-1} . m/z = 967 ($\text{M}^+ - \text{H}_2\text{O}$, $\text{C}_2\text{H}_5\text{OH}$) + Na.

Synthesis of $\text{Gd}(\text{PBI})_3\cdot 2\text{H}_2\text{O}$. An aqueous solution of $\text{Gd}(\text{NO}_3)_3\cdot 6\text{H}_2\text{O}$ (0.5 mmol) was added to a solution of HPBI (1.5 mmol) in ethanol in the presence of NaOH (1.5 mmol). Precipitation took place immediately, and the reaction mixture was stirred for 10 h at room temperature. The product was filtered, washed with ethanol, with water, and then with ethanol, and dried and stored in a desiccator. The complex was then purified by recrystallization from dichloromethane–ethanol mixture. Elemental analysis (%): Calcd for $\text{C}_{48}\text{H}_{34}\text{GdN}_3\text{O}_{11}$ (986.06): C, 58.46; H, 3.45; N, 4.26. Found: C, 58.40; H, 3.61; N, 4.24. IR (KBr) ν_{max} : 3300, 1640, 1612, 1483, 1389, 1184, 910 cm^{-1} . m/z = 950 ($\text{M}^+ - 2\text{H}_2\text{O}$).

Synthesis of Complexes 2–5. Synthesis routes of the complexes **2–5** are shown in Scheme 2. All these complexes were prepared by stirring equimolar solutions of $\text{Eu}(\text{PBI})_3\cdot\text{C}_2\text{H}_5\text{OH}\cdot\text{H}_2\text{O}$ and nitrogen donors in CHCl_3 for 24 h at room temperature. The products were obtained after solvent evaporation and are purified by recrystallization from dichloromethane–ethanol mixture.

$\text{Eu}(\text{PBI})_3\cdot\text{bpy}$ (2). Elemental analysis (%): Calcd for $\text{C}_{58}\text{H}_{38}\text{EuN}_5\text{O}_9$ (1100.19): C, 63.32; H, 3.48; N, 6.37. Found: C, 62.99; H, 3.54; N, 6.08. IR (KBr) ν_{max} : 1638, 1605, 1602, 1483, 1389, 910, 760 cm^{-1} . m/z = 1123.3 (M^+) + Na.

$\text{Eu}(\text{PBI})_3\cdot\text{dmbpy}$ (3). Elemental analysis (%): Calcd for $\text{C}_{60}\text{H}_{42}\text{EuN}_5\text{O}_{11}$ (1160.19): C, 62.12; H, 3.65; N, 6.04. Found: C, 61.98; H, 3.61; N, 6.47. IR (KBr) ν_{max} : 1640, 1607, 1603, 1483, 1434, 1388, 1182, 1024 cm^{-1} . m/z = 1183.7 (M^+) + Na.

$\text{Eu}(\text{PBI})_3\cdot\text{phen}$ (4). Elemental analysis (%): Calcd for $\text{C}_{60}\text{H}_{38}\text{EuN}_5\text{O}_9$ (1124.96): C, 64.06; H, 3.4; N, 6.23. Found: C, 63.91; H, 3.39; N, 6.53. IR (KBr) ν_{max} : 1638, 1605, 1600, 1482, 1434, 1388, 1182, 1024 cm^{-1} . m/z = 1148.5 (M^+) + Na.

$\text{Eu}(\text{PBI})_3\cdot\text{bath}$ (5). Elemental analysis (%): Calcd for $\text{C}_{60}\text{H}_{38}\text{EuN}_5\text{O}_9$ (1277.15): C, 67.71; H, 3.63; N, 5.48. Found: C, 67.68;

H, 3.69; N, 76. IR (KBr) ν_{max} : 1637, 1607, 1601, 1483, 1437, 1182, 1021, 906 cm^{-1} . m/z = 1300.47 (M^+) + Na.

Results and Discussion

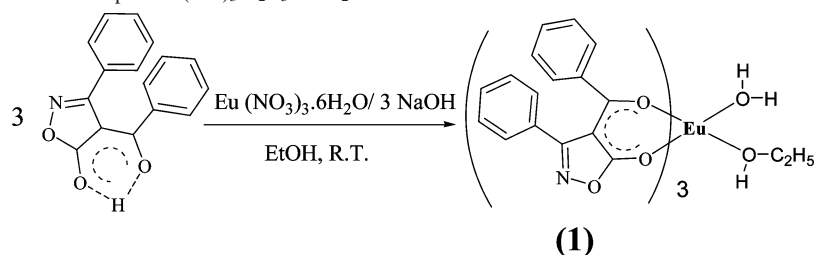
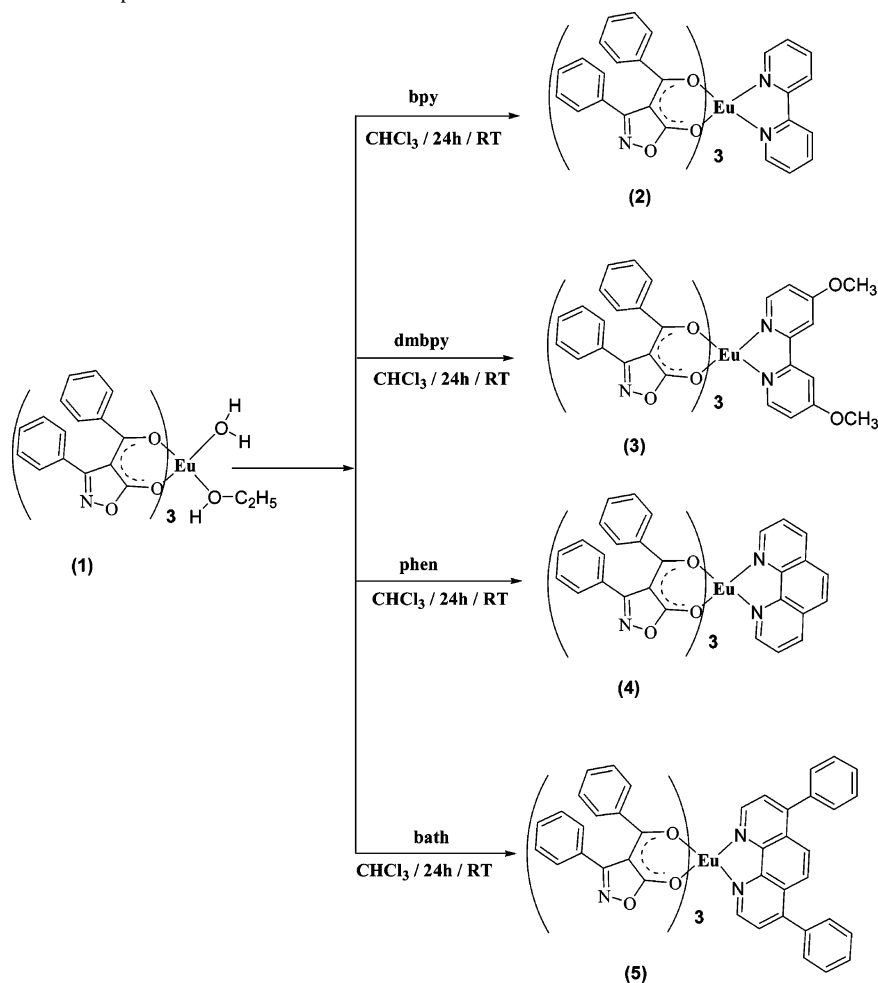
Structural Characterization of Europium(III) Complexes. The synthesis procedure of europium complexes **1–5** is shown in Schemes 1 and 2. The microanalyses and HRMS studies of complexes **1–5** show that Eu^{3+} ion has reacted with HPBI in a metal-to-ligand mole ratio of 1:3 and one molecule of bidentate nitrogen ligand is involved in complexes **2–5**. The IR spectrum of complex **1** shows a broad absorption in the region 3000–3500 cm^{-1} , indicating the presence of solvent molecules in the complex. The existence of solvent molecules in lanthanide complexes with heterocyclic β -diketones such as 1-phenyl-3-methyl-4-acylpyrazolones is well documented.^{21,22} On the other hand, the absence of the broad band in the region 3000–3500 cm^{-1} for complexes **2–5** suggests that water and solvent molecules have been displaced by the bidentate nitrogen donors. The carbonyl stretching frequency of HPBI (1699 cm^{-1}) has been shifted to lower wavenumbers in complexes **1–5** (1641 cm^{-1} in **1**; 1638 cm^{-1} in **2**; 1640 cm^{-1} in **3**; 1640 cm^{-1} in **4**; 1637 cm^{-1} in **5**), indicating the involvement of carbonyl oxygen in the complex formation with Eu^{3+} ion. Further, the red shifts observed in the C=N stretching frequencies of nitrogen donors (1615 cm^{-1}) in complexes **2–5** (to 1605 cm^{-1} in **2**; 1607 cm^{-1} in **3**; 1605 cm^{-1} in **4**; 1607 cm^{-1} in **5**) show the involvement of nitrogen in the complex formation with Eu^{3+} ion.

It is clear from the thermogravimetric analysis data that complex **1** (Figure S1 in Supporting Information) undergoes a mass loss of 7% (calculated: 6.3%) up to 150 °C, which corresponds to the removal of coordinated solvent molecules. On the other hand, in complexes **2–5** (Figures S2–S4 in Supporting Information) there is no mass loss up to 200 °C, indicating the absence of solvent molecule in the coordination sphere. Further, decomposition takes place in the region 200–800 °C for all the complexes.

The structure of $\text{Eu}(\text{PBI})_3\cdot\text{H}_2\text{O}\cdot\text{EtOH}$ (**1**) and $\text{Eu}(\text{PBI})_3\cdot\text{phen}$ (**4**) were characterized by single-crystal X-ray crystallography. Details of crystal data and data collection parameters for complexes **1** and **4** are given in Table 1. The selected bond lengths and bond angles for complexes are listed in Table 2. The asymmetric unit of $\text{Eu}(\text{PBI})_3\cdot\text{H}_2\text{O}\cdot\text{EtOH}$ is shown in Figure 1, and crystal packing is shown in Figure 2. The central Eu^{3+} ion is coordinated with eight oxygen atoms: six from the three bidentate HPBI ligands, one from a water molecule, and another from an ethanol molecule. The coordination geometry of the metal center is best described as a bicapped trigonal prism. The average bond length between the europium ion and the isoxazolone oxygen atoms is 2.395 Å, which is slightly shorter than that of europium and water oxygen atom (2.399 Å) and also that

(21) Pettinari, C.; Marchetti, F.; Cingolanni, A.; Drozdov, A.; Timokhin, I.; Troyanov, S. I.; Tsaryuk, V.; Zolin, V. *Inorg. Chim. Acta* **2004**, 357, 4181–4190.

(22) Shen, L.; Shi, M.; Li, F.; Zhang, D.; Li, X.; Shi, E.; Yi, T.; Du, Y.; Huang, C. *Inorg. Chem.* **2006**, 45, 6188–6197.

Scheme 1. Synthesis Route of the Complex $\text{Eu}(\text{PBI})_3 \cdot \text{C}_2\text{H}_5\text{OH} \cdot \text{H}_2\text{O}$ **Scheme 2.** Synthesis Route for Complexes 2–5**Table 2.** Selected Bond Lengths (Å) and Angles (deg) for Complexes 1 and 4

1		4	
Eu–O(1)	2.457(2)	Eu–O(1)	2.378(4)
Eu–O(2)	2.373(2)	Eu–O(2)	2.361(4)
Eu–O(4)	2.388(2)	Eu–O(4)	2.385(4)
Eu–O(5)	2.382(3)	Eu–O(5)	2.376(4)
Eu–O(7)	2.330(2)	Eu–O(7)	2.441(3)
Eu–O(8)	2.438(2)	Eu–O(8)	2.340(4)
Eu–O(10)	2.469(2)	Eu–N(4)	2.550(4)
Eu–O(11)	2.399(3)	Eu–N(5)	2.614(4)
O(1)–Eu–O(2)	73.45(8)	O(1)–Eu–O(2)	71.47(13)
O(4)–Eu–O(5)	71.12(8)	O(4)–Eu–O(5)	72.32(13)
O(7)–Eu–O(8)	72.28(8)	O(7)–Eu–O(8)	71.65(12)
O(10)–Eu–O(11)	144.17(3)	N(4)–Eu–N(5)	63.67(14)

of europium and ethanol oxygen atom (2.469 Å). This may be due to the result of the negative charge of the isoxazolone oxygen, which could be more strongly coordinated to the

europium ion due to electrostatic effects. Similar behavior has been reported elsewhere in the X-ray single-crystal structure of $\text{Tb}(\text{PMPP})_3 \cdot 2\text{H}_2\text{O}$ (where PMPP = 1-phenyl-3-methyl-4-propionyl-5-pyrazolone).²³ The ethanol molecule coordinating to the cation donates a hydrogen bond to a nitrogen atom of a ligand molecule of a neighboring cluster [$\text{N}(3) \cdots \text{O}(10) = 2.913(2)$], and pairs of complex molecules are linked by two of these bonds as shown in Figure 2a. The disordered ethanol molecule accepts one hydrogen bond from the water molecule coordinating the cation [$\text{O}(11)_{\text{water}} \cdots \text{O}(12)_{\text{ethanol}} = 2.702(2)$] and donates a bond to a ligand nitrogen atom of a neighboring cluster [$\text{O}(12)_{\text{ethanol}} \cdots \text{N}(2) = 2.913(2)$] to form bridges between pairs of clusters (Figure 2b). The water molecule also hydrogen bonds with a nitrogen

(23) Zhou, D.; Li, Q.; Huang, C.; Yao, G.; Umetani, S.; Matsui, M.; Ying, L.; Yu, A.; Zhao, X. *Polyhedron* **1997**, 16, 1381–1389.

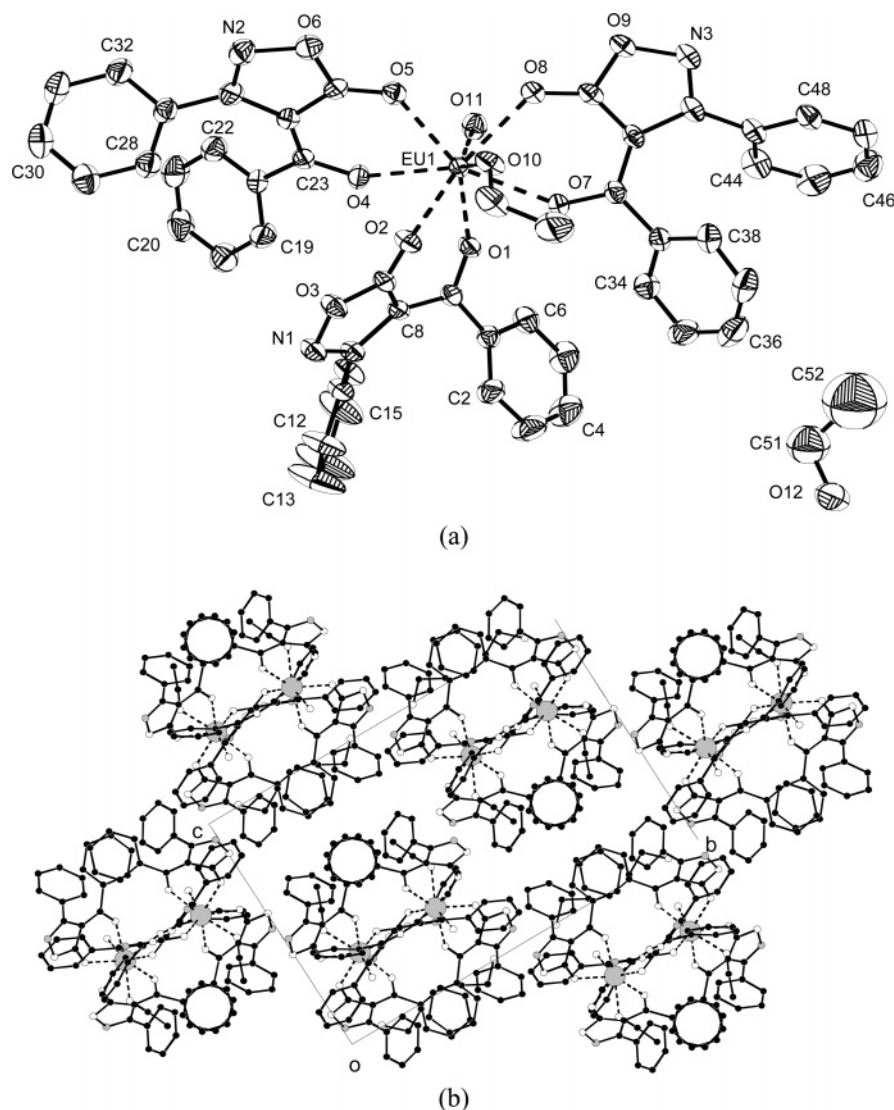


Figure 1. (a) Asymmetric unit and (b) crystal packing viewed down the axis of complex **1**. Hydrogen atoms have been omitted for clarity.

atom of a neighboring cluster $[\text{N}(1) \cdots \text{O}(11)]_{\text{water}} = 2.809$ –(2)] to form chains parallel to the a -axis.

In complex **4**, the central Eu^{3+} ion is coordinated by six oxygen atoms from three HPBI ligands and two nitrogen atoms from a bidentate phenanthroline ligand, resulting in a coordination number of eight. The coordination geometry can be described as a distorted square antiprism with six oxygen atoms and two nitrogen atoms (Figure 3). A similar geometric structure was reported elsewhere for the tris(acetylacetonate)europium(III) phenanthroline and tris(dibenzolmethanido)europium(III) phenanthroline complexes by single-crystal X-ray diffraction studies.²⁴ The average Eu–N bond distance (2.58 Å) is longer than the Eu–O bonds of HPBI ligands (2.34–2.44 Å), as observed in the X-ray single-crystal data of the complex tris(4,4,5,5,6,6,6-heptafluoro-1-(2-naphthyl)hexane-1,3-dione)europium(III) with phenanthroline (Eu–O bonds 2.34–2.40 Å in HFNH; Eu–N, 2.60 Å in phen)²⁵ and tris(dibenzolmethanido)europium(III) phenan-

throline (Eu–O bonds 2.31–2.41 Å in DBM; Eu–N, 2.66 Å in phen).²⁴

UV–Vis Spectra. UV–vis absorption spectra of the ligands (HPBI, bpy, dmbpy, phen, bath) and their Eu(III) complexes measured in CH_3CN ($c = 2 \times 10^{-5}$ M) are shown in Figures 4 and 5, respectively. The maximum absorption band at 316 nm for HPBI, 311 nm for complex **1**, and the hump observed around 311 nm in complexes **2–5** are attributed to singlet–singlet $\pi \rightarrow \pi^*$ enol absorption of heterocyclic β -diketonate. Compared with the ligand HPBI ($\lambda_{\text{max}} = 316$ nm), the absorption maxima are blue shifted to 311 nm in complexes **1–5**. The absorption maxima at 290, 298, 289, and 289 nm in complexes **2**, **3**, **4**, and **5**, respectively, are due to the $^1\pi \rightarrow \pi^*$ absorption of the aromatic rings of bidentate nitrogen donors. These values also shows a blue shift of 1, 1, 9, and 12 nm, respectively, in complexes compared to free nitrogen donors (291, 299, 298, and 301 nm). The spectral shapes of the complexes in CH_3CN are similar to that of the free ligands, suggesting that the coordination of Eu^{3+} ion does not have a significant influence on the $^1\pi \rightarrow \pi^*$ state energy. However, a small blue shift

(24) Ahmed, M. O.; Liao, J. L.; Chen, X.; Chen, S. A.; Kaldis, J. H. *Acta Crystallogr.* **2003**, *E59*, m29–m32.

(25) Yu, J.; Zhou, L.; Zhang, H.; Zheng, Y.; Li, H.; Deng, R.; Peng, Z.; Li, Z. *Inorg. Chem.* **2005**, *44*, 1611–1618.

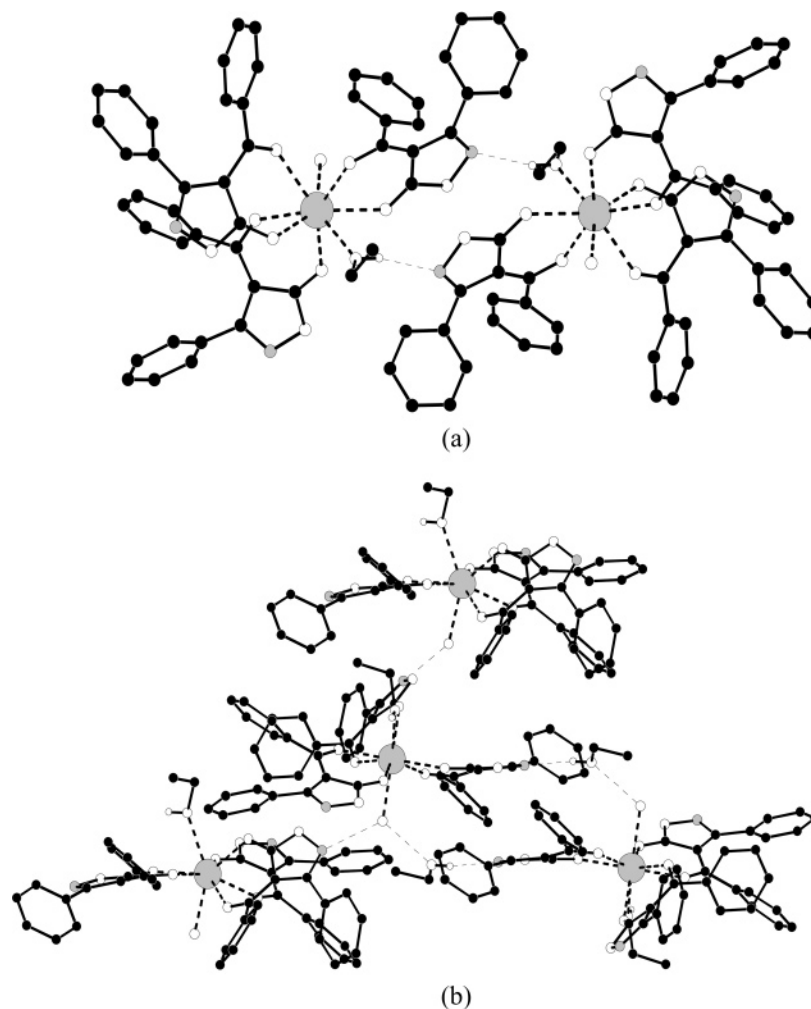


Figure 2. (a) Linkage of clusters by ethanol molecules and (b) hydrogen bonding involving water molecules. Some hydrogen atoms have been omitted for clarity.

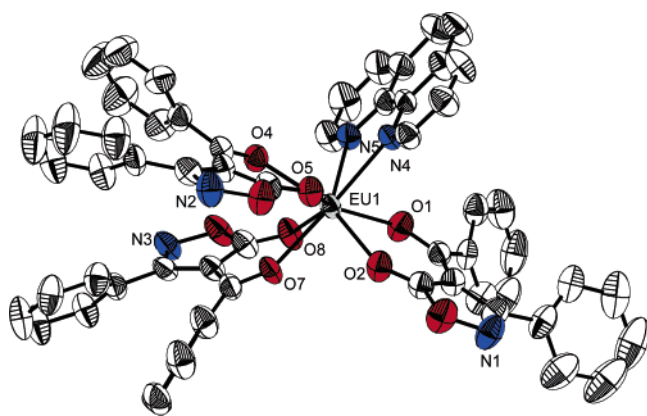


Figure 3. Asymmetric unit of complex 4.

observed in the absorption maximum of all the complexes is due to the perturbation induced by the metal coordination. The determined molar absorption coefficient values of the complexes **1**, **2**, **3**, **4**, and **5** at 311 nm, 2.82×10^4 , 2.94×10^4 , 2.90×10^4 , 2.92×10^4 , and 2.96×10^4 L mol⁻¹ cm⁻¹, respectively, are about 3 times higher than that of the HPBI (9.4×10^3 at 316 nm), indicating the presence of three β -diketonate ligands in the corresponding complexes. Further, the higher molar absorption coefficient of HPBI reveals that the β -diketonate ligand has a strong ability to absorb light.

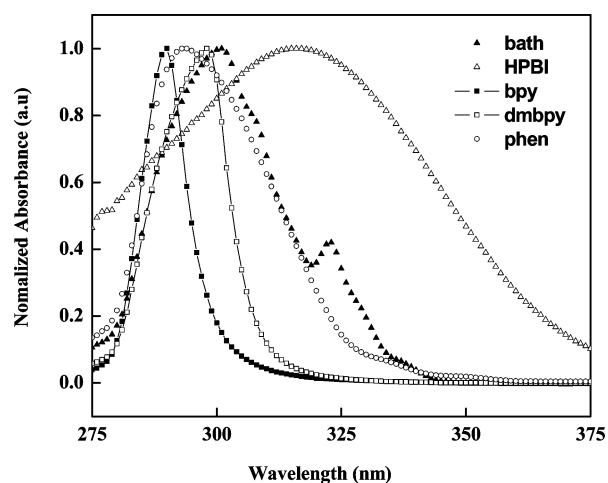


Figure 4. UV-visible absorption spectra of ligands in acetonitrile ($c = 2 \times 10^{-5}$ M).

PL Properties of Complexes 1–5. The normalized excitation spectra of the europium complexes **1–5** (in solid state) at room temperature, monitored around the peak of the intense $^5D_0 \rightarrow ^7F_2$ transition of the Eu³⁺ ion, are shown in Figure 6. The excitation spectra of all the complexes exhibit a broad band between 250 and 450 nm and a series of sharp lines characteristic of the Eu³⁺ energy level structure,

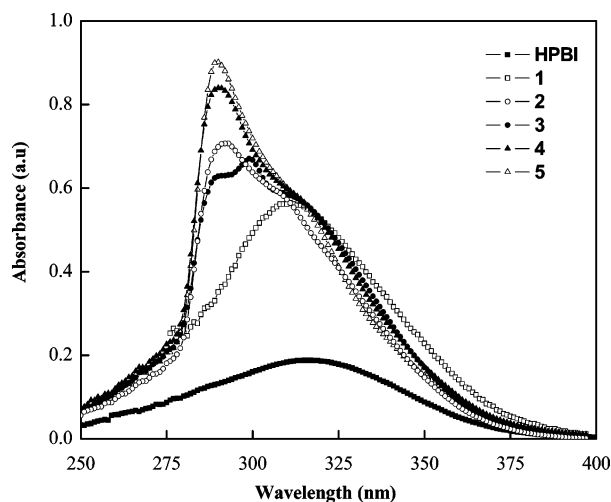


Figure 5. UV-visible absorption spectra of HPBI and complexes **1–5** in acetonitrile ($c = 2 \times 10^{-5}$ M).

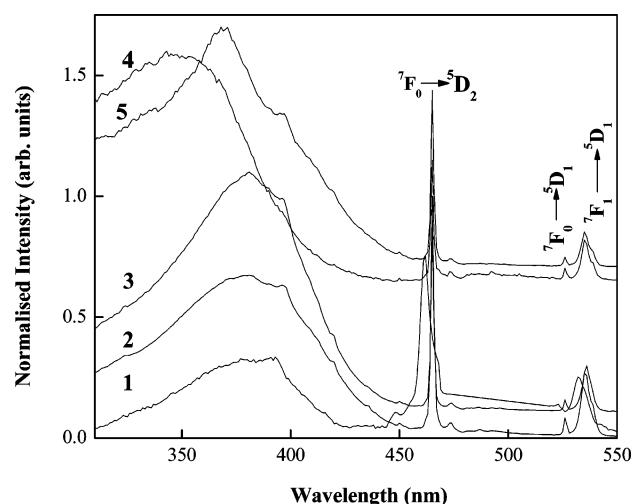


Figure 6. Excitation spectrum of $^5\text{D}_0$ emission ($\lambda_{\text{max}} = 613$ nm) of Eu^{3+} complexes **1–5** at 303 K.

assigned to transitions between the $^7\text{F}_{0,1}$ and the $^5\text{L}_6$, $^5\text{D}_{3,2,1}$ levels. This transition is weaker than the absorption of the organic ligands and is overlapped by a broad excitation band, which proves that luminescence sensitization via excitation of the ligand is much more efficient than the direct excitation of the Eu^{3+} ion absorption level. The broad band may be related to the excited states of ligands or to the ligand-to-metal charge transfer (LMCT) transitions resulting from the interaction between the ion and the ligand's first coordination shell.^{5,26}

The room-temperature normalized emission spectra of europium complexes **1–5** (in solid state) under the excitation wavelengths that maximize the Eu^{3+} emission intensity are shown in Figure 7. The emission spectra of the europium complexes display characteristic sharp peaks in the 575–725 nm region associated with the $^5\text{D}_0 \rightarrow ^7\text{F}_j$ transitions of the Eu^{3+} ion. The five expected peaks for the $^5\text{D}_0 \rightarrow ^7\text{F}_{0-4}$ transitions are well resolved and the hypersensitive $^5\text{D}_0 \rightarrow ^7\text{F}_2$ transition is very intense, pointing to a highly polarizable

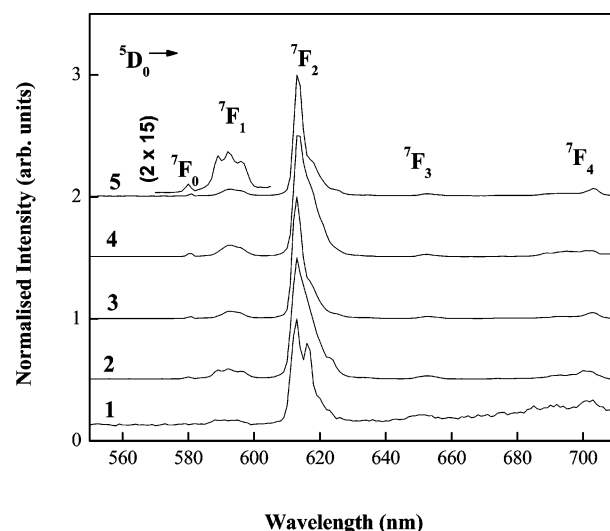


Figure 7. Room-temperature PL spectrum of complexes **1–5** excited at their maximum emission wavelengths (367, 369, 371, 350, and 360 nm, respectively, for complexes **1**, **2**, **3**, **4**, and **5**).

chemical environment around the Eu^{3+} ion that is responsible for the brilliant red emission of these complexes. A relevant feature that may be noted for complexes **1–5** is the very high intensity of the $^5\text{D}_0 \rightarrow ^7\text{F}_2$ transition, relative to the $^5\text{D}_0 \rightarrow ^7\text{F}_1$ lines, indicating that the Eu^{3+} ion coordinated in a local site without an inversion center. Further, the emission spectra of the complexes show only one peak for $^5\text{D}_0 \rightarrow ^7\text{F}_0$ transition and three stark components for the $^5\text{D}_0 \rightarrow ^7\text{F}_1$ transition, indicating the presence of a single chemical environment around the Eu^{3+} ion.

The lifetime values (τ_{obs}) of the $^5\text{D}_0$ level were determined from the luminescence decay profiles for complexes **1–5** at room temperature by fitting with a monoexponential curve, and they are depicted in Table 3. Typical decay profiles of complexes **2–5** are shown in Figure S6 (Supporting Information). The relatively shorter lifetime obtained for complex **1** may be due to dominant nonradiative decay channels associated with vibronic coupling due to the presence of solvent molecules, as is well documented for many of the hydrated europium β -diketonate complexes.⁵ Longer lifetime values have been observed for complexes **2–5** compared to complex **1**, due to the absence of nonradiative pathways.

Judd–Ofelt theory is a useful tool for analyzing f–f electronic transitions.²⁷ Interaction parameters of ligand fields are given by the Judd–Ofelt parameters Ω_λ (where $\lambda = 2, 4, \text{ and } 6$). In particular, Ω_2 is more sensitive to the symmetry and sequence of ligand fields. To produce faster Eu^{3+} radiation rates, antisymmetrical Eu^{3+} complexes with larger Ω_2 parameters need to be designed. The experimental Ω_2 and Ω_4 intensity parameters were determined from the emission spectra given in Figure 7 by using the $^5\text{D}_0 \rightarrow ^7\text{F}_2$ and $^5\text{D}_0 \rightarrow ^7\text{F}_4$ electronic transitions, respectively, and by expressing the emission intensity $I_j = \hbar\omega_{j0}A_{\text{RAD}}(J)N(^5\text{D}_0)$ in terms of the area under the emission curve. Here $\hbar\omega_{j0}$ is the transition energy and N is the population of the $^5\text{D}_0$ level.

(26) Braga, S. S.; Ferreira, R. S.; Goncalves, I. S.; Pillinger, M.; Rocha, J.; Teixeira-Dias, J. C.; Carlos, L. D. *J. Phys. Chem. B* **2004**, *106*, 11430–11437.

(27) (a) Judd, B. R. *Phys. Rev.* **1962**, *127*, 750–761. (b) Ofelt, G. S. *J. Chem. Phys.* **1962**, *37*, 511–519. (c) Werts, M. H. V.; Jukes, R. T. F.; Verhoeven, W. *J. Phys. Chem. Chem. Phys.* **2002**, *4*, 1542–1548.

Table 3. Experimental Intensity Parameters ($\Omega_{2,4}$), R_{02} , Radiative (A_{RAD}) and Nonradiative (A_{NR}) Decay Rates, $^5\text{D}_0$ Lifetime (τ_{obs}), Intrinsic Quantum Yields (Φ_{Ln} , %; Φ_{transfer} , %), and Overall Quantum Yield (Φ_{overall} , %) for Complexes **1–5** at 303 K

complex	$10^{-20}\Omega_2$ (cm ²)	$10^{-20}\Omega_4$ (cm ²)	R_{02}	A_{RAD} (s ⁻¹)	A_{NR} (s ⁻¹)	τ_{obs} (μs)	Φ_{Ln} (%)	Φ_{transfer} (%)	Φ_{overall} (%)
1	26.47	14.29	0.0097	1059	2941	250	26	8.0	2.2
2	19.25	3.22	0.0063	6911	3314	978	68	22	15
3	17.25	1.91	0.0082	6094	2373	1181	72	25	18
4	15.66	1.53	0.0072	5543	4213	1025	57	20	11
5	20.19	2.06	0.0054	7023	2878	1010	71	22	15

The radiative emission rates, $A_{\text{RAD}}(J)$, are given by^{28,29}

$$A_{\text{RAD}} = \frac{4e^2\omega^3}{3\hbar c^3} \chi \sum_{\lambda} \Omega_{\lambda} \langle {}^7\text{F}_J || U^{(\lambda)} || {}^5\text{D}_0 \rangle^2 \frac{1}{2J+1} \quad (2)$$

where e is the electronic charge, ω is the angular frequency of the transition, \hbar is Planck's constant over 2π , c is the velocity of light, χ is the Lorentz local field correction term given by $n(n^2 + 2)^2/9$, n being the refraction index, and $\langle {}^7\text{F}_J || U^{(\lambda)} || {}^5\text{D}_0 \rangle^2$ are the squared reduced matrix elements whose values are 0.0032 and 0.0023 for $J = 2$ and 4 , respectively.³⁰ The magnetic dipole allowed $^5\text{D}_0 \rightarrow {}^7\text{F}_1$ transition was taken as reference,^{28,31} in vacuo $A_{\text{RAD}}(^5\text{D}_0 \rightarrow {}^7\text{F}_1) = 14.65 \text{ s}^{-1}$.²⁶ An average index of refraction equal to 1.5 was considered, leading to $A_{\text{RAD}}(^5\text{D}_0 \rightarrow {}^7\text{F}_1) \approx 50 \text{ s}^{-1}$.³² The Ω_6 parameter was not determined since the $^5\text{D}_0 \rightarrow {}^7\text{F}_{5,6}$ transitions could not be experimentally detected. Table 3 lists the Ω_2 and Ω_4 intensity parameters estimated for complexes **1–5**. A point to be noted in these results is the relatively high values of the Ω_2 parameter for complexes **1–5**. This might be interpreted as being a consequence of the hypersensitive behavior of the $^5\text{D}_0 \rightarrow {}^7\text{F}_2$ transition.³³ The dynamic coupling mechanism is, therefore, dominant, indicating that the Eu^{3+} ion is in a highly polarizable chemical environment.

The overall quantum yield (Φ_{overall}) of the europium complex treats the complex as a “black box” where the internal process is not explicitly considered: given that the complex absorbs a photon (i.e., the antenna is excited), the overall quantum yield can be defined as³⁴

$$\Phi_{\text{overall}} = \Phi_{\text{transfer}} \Phi_{\text{Ln}} \quad (3)$$

Here Φ_{transfer} is the efficiency of energy transfer from the ligand to Eu^{3+} and Φ_{Ln} is the intrinsic quantum yield of the lanthanide ion. The latter can be calculated as

$$\Phi_{\text{Ln}} = \frac{A_{\text{RAD}}}{A_{\text{RAD}} + A_{\text{NR}}} \quad (4)$$

$$\tau_{\text{obs}} = \frac{1}{A_{\text{RAD}} + A_{\text{NR}}} \quad (5)$$

where A_{RAD} and A_{NR} are the radiative and nonradiative decay rates, respectively. A_{RAD} can be calculated using eq 2, and the nonradiative rates A_{NR} can be obtained from the calculated A_{RAD} and the observed lifetime (τ_{obs}) using eq 5.

Table 3 gives the overall quantum yield (Φ_{overall}), A_{RAD} and A_{NR} , intrinsic quantum yield (Φ_{Ln}), and Φ_{transfer} values for complexes **1–5**. The R_{02} intensity parameter, defined as the ratio between the intensities of the $^5\text{D}_0 \rightarrow {}^7\text{F}_0$ and $^5\text{D}_0 \rightarrow {}^7\text{F}_2$ transitions, gives information on the J -mixing effect associated with $^5\text{D}_0 \rightarrow {}^7\text{F}_0$ transition and is also given in Table 3. According to energy gap theory, radiationless transitions are prompted by ligands and solvents with high-frequency vibrational modes. Creation of Eu^{3+} complexes with higher quantum yields is directly linked to suppression of radiationless transitions caused by vibrational excitations in surrounding media.^{14,35–37} It is clear from Table 3 that complex **1**, having solvent molecules in the coordination sphere, exhibits a lower quantum yield. This is due to the presence of O–H oscillators in this system, which effectively quench the luminescence of the Eu^{3+} ion. On the other hand, complexes **2–5** exhibit high quantum yield and lifetime values due to the displacement of solvent molecules from the coordination sphere by the bidentate nitrogen donors. Among complexes **2** and **3**, the latter shows a better quantum yield due to the enhanced basicity of the coordinating nitrogen atoms upon the substitution of two electron-donating groups (OCH_3) in the para,para'-position in the bipyridine molecule. On the other hand, among complexes **4** and **5**, again the latter exhibits a high quantum yield due to the extended conjugation obtained by the introduction of two phenyl groups in the 4,7-positions of the phenanthroline ligand. The intrinsic quantum yield and $^5\text{D}_0$ lifetime obtained in the present study for the Eu^{3+} complexes **2–5** were found to be promising when compared to that observed for the various Eu^{3+} β -diketonate–bidentate nitrogen donor complexes reported so far in the literature (Table 4).

Energy Transfer between Ligands and Eu^{3+} . To demonstrate the energy transfer process, the phosphorescence

- (28) Malta, O. L.; Brito, H. F.; Menezes, J. F. S.; Gonçalves e Silva, F. R.; Alves, S., Jr.; de Andrade, A. M. V. *J. Lumin.* **1997**, *75*, 255–268.
- (29) Malta, O. L.; dos Santos, M. A. C.; Thompson, L. C.; Ito, N. K. *J. Lumin.* **1996**, *69*, 77–84.
- (30) Carnall, W. T.; Crosswhite, H. M. *Energy levels, Structure and Transition Probabilities of the Trivalent Lanthanides in LaF₃*; Argonne National Laboratory: IL, 1977.
- (31) Carlos, L. D.; Messaddeq, Y.; Brito, H. M.; Sá Ferreira, R. A.; V. de Zea Bermudez, V.; Ribeiro, S. J. L. *Adv. Mater.* **2000**, *12*, 594–598.
- (32) Molina, C.; Moreira, P. J.; Gonçalves, R. R.; Sá Ferreira, R. A.; Messaddeq, Y.; Ribeiro, S. J. L.; Soppera, O.; Leite, A. P.; Marques, P. V. S.; de Zea Bermudez, V.; Carlos, L. D. *J. Mater. Chem.* **2005**, *15*, 3937–3945.
- (33) Peacock, R. D. *Struct. Bonding (Berlin)* **1975**, *22*, 83–121.
- (34) (a) Xiao, M.; Selvin, P. R. *J. Am. Chem. Soc.* **2001**, *123*, 7067–7073. (b) Comby, S.; Imbert, D.; Anne-Sophie, C.; Bunzli, J. C. G.; Charvonnier, L. J.; Ziessel, R. F. *Inorg. Chem.* **2004**, *43*, 7369–7379. (c) Quici, S.; Cavazzini, M.; Marzanni, G.; Accorsi, G.; Armaroli, N.; Ventura, B.; Barigelletti, F. *Inorg. Chem.* **2005**, *44*, 529–537.

- (35) Peng, C.; Zhang, H.; Yu, J.; Meng, Q.; Fu, L.; Li, H.; Sun, L.; Guo, X. *J. Phys. Chem. B* **2005**, *109*, 15278–15287.
- (36) Wada, Y.; Ohkubo, T.; Ryo, M.; Nakarawa, T.; Hasegawa, Y.; Yanagida, S. *J. Am. Chem. Soc.* **2000**, *122*, 8583–8584.
- (37) Hasegawa, Y.; Ohkubo, T.; Sogabe, K.; Kawamura, Y.; Wada, Y.; Nakashima, N.; Yanagida, S. *Angew. Chem., Int. Ed.* **2000**, *39*, 357–360.

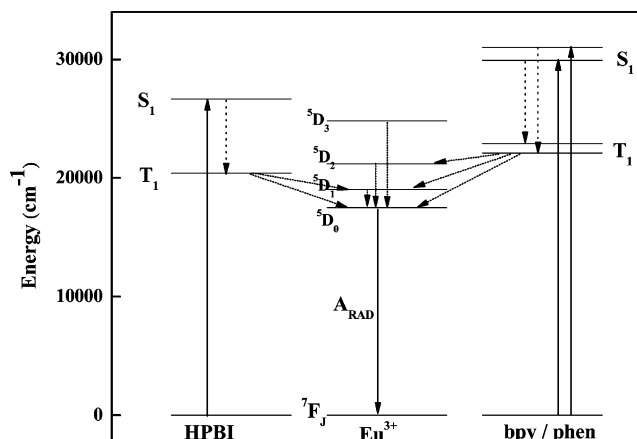
Table 4. Solid State Photophysical Data for $^5\text{D}_0$ Luminescence of Some Selected Eu^{3+} Complexes at Room Temperature

complex ^a	A_{RAD} (s^{-1})	A_{NR} (s^{-1})	τ_{obs} (μs)	Φ_{Ln} (%)
$\text{Eu}(\text{PBI})_3\cdot\text{phen}$	5543	4213	1025	57
$\text{Eu}(\text{PBI})_3\cdot\text{bpy}$	6911	3314	978	68
$\text{Eu}(\text{tta})_3\cdot\text{phen}^{35}$	436	993	700	31
$\text{Eu}(\text{btfa})_3\cdot\text{phen}^5$	580	569	210	50
$\text{Eu}(\text{NTA})_3\cdot\text{phen}^{38}$	600	900	662	40
$\text{Eu}(\text{NTA})_3\cdot\text{bpy}^{39}$	816	797	620	51

^a tta = 2-thenoyltrifluoroacetate; btfa = 4,4,4-trifluoro-1-phenyl-1,3-butanedionate; NTA = 1-(2-naphthoyl)-3,3,3-trifluoroacetate.

spectra of the complex $\text{Gd}(\text{PBI})_3\cdot 2\text{H}_2\text{O}$ was measured for the triplet energy level data of the ligand HPBI. From the phosphorescence spectra (Figure S7 in the Supporting Information), the triplet energy level ($^3\pi\pi^*$) of $\text{Gd}(\text{PBI})_3\cdot 2\text{H}_2\text{O}$, which corresponds to its peak emission wavelength, is $20\,366\text{ cm}^{-1}$ (491 nm). Because the lowest excited state $^6\text{P}_{7/2}$ of Gd^{3+} is too high to accept energy from a ligand, the data obtained from the phosphorescence spectra actually reveal the triplet energy level of HPBI in europium complexes. The singlet state energy ($^1\pi\pi^*$) level of HPBI is estimated by referencing its absorbance edge, which is $27\,397\text{ cm}^{-1}$ (365 nm). The singlet and triplet energy levels of bpy (29 900 and $22\,900\text{ cm}^{-1}$) and phen (31 000 and $22\,100\text{ cm}^{-1}$) were taken from the literature.⁴⁰

In general, the sensitization pathway in luminescent europium complexes consists of excitation of the ligands into their excited singlet states, subsequent intersystem crossing of the ligands to their triplet states, and the energy transfer from the triplet state to the $^5\text{D}_J$ manifold of the Eu^{3+} ions, followed by internal conversion to the emitting $^5\text{D}_0$ state. Finally, the Eu^{3+} ion emits when transition to the ground state occurs.¹⁶ Moreover, the electron transition from the higher excited states, such as $^5\text{D}_3$ ($24\,800\text{ cm}^{-1}$), $^5\text{D}_2$ ($21\,200\text{ cm}^{-1}$), and $^5\text{D}_1$ ($19\,000\text{ cm}^{-1}$), to $^5\text{D}_0$ ($17\,500\text{ cm}^{-1}$) becomes feasible by internal conversion, and most of the photophysical processes take place in this orbital. Consequently, most europium complexes give rise to typical emission bands at ~ 581 , 593, 614, 654, and 702 nm corresponding to the deactivation of the excited state $^5\text{D}_0$ to the ground states $^7\text{F}_J$ ($J = 0-4$). Thus, matching the energy levels of the triplet state of the ligands to $^5\text{D}_0$ of Eu^{3+} is one of the key factors that affect the luminescent properties of the europium complexes. Based on the above experimental results, the energy level diagram and the possible energy transfer pathways are shown in Figure 8. The triplet energy levels of HPBI ($20\,366\text{ cm}^{-1}$), bpy ($22\,900\text{ cm}^{-1}$), and phen ($22\,100\text{ cm}^{-1}$) are higher than the $^5\text{D}_0$ level ($17\,500\text{ cm}^{-1}$) of Eu^{3+} , and their energy gaps $\Delta E(^3\pi\pi^* - ^5\text{D}_0)$ between ligand and metal-centered levels are too high to allow an effective back energy transfer. According to Latva's empirical rule,⁴¹ an optimal ligand-to-metal energy transfer process for Eu^{3+}

**Figure 8.** Schematic energy level diagram and the energy transfer process: S_1 , first excited singlet state; T_1 , first excited triplet state.

needs $\Delta E(^3\pi\pi^* - ^5\text{D}_0) > 2500\text{ cm}^{-1}$ and hence the energy transfer process is effective for complexes **1–5**. It is also noted that the energy gaps between the $^1\pi\pi^*$ and $^3\pi\pi^*$ levels are 7031, 7000, and 8900 cm^{-1} for HPBI, bpy, and phen, respectively. According to Reinhoudt's empirical rule, the intersystem crossing process becomes effective when $\Delta E(^1\pi\pi^* - ^3\pi\pi^*)$ is at least 5000 cm^{-1} ;⁴² thus HPBI, bpy, and phen are effective sensitizers for Eu^{3+} and the intersystem crossing processes in complexes **1–5** are effective.

Conclusions

The photophysical properties of new heterocyclic β -diketonate europium complexes $\text{Eu}(\text{PBI})_3\cdot\text{H}_2\text{O}\cdot\text{EtOH}$ (**1**), $\text{Eu}(\text{PBI})_3\cdot\text{bpy}$ (**2**), $\text{Eu}(\text{PBI})_3\cdot\text{dmbpy}$ (**3**), $\text{Eu}(\text{PBI})_3\cdot\text{phen}$ (**4**), and $\text{Eu}(\text{PBI})_3\cdot\text{bath}$ (**5**) were investigated. For the first time the single-crystal X-ray structures of novel europium-3-phenyl-4-benzoyl-5-isoxazolonate complexes were established. The sensitization mechanism for luminescent europium complexes involves a usual triplet pathway, in which the transfer of energy absorbed by the ligand to the Eu^{3+} ion takes place from the ligand-centered triplet excited state. The characteristic emission spectra of Eu^{3+} complexes show a very high intensity for the hypersensitive $^5\text{D}_0 \rightarrow ^7\text{F}_2$ transition, pointing to a highly polarizable chemical environment around the Eu^{3+} ion. The results show that the substitution of solvent molecules by bidentate nitrogen ligands in $\text{Eu}(\text{PBI})_3\cdot\text{H}_2\text{O}\cdot\text{EtOH}$ complex greatly enhances the metal-centered luminescence quantum yields and lifetime values. The intrinsic luminescent quantum yields of Eu^{3+} ion in complexes **2–4** are in the range 57–72%, and these values are promising,

(38) Fernandes, J. A.; Ferreira, R. A. S.; Pillinger, M.; Carlos, L. D.; Jepsen, J.; Hazell, A.; Ribeiro-Claro, P.; Gonçalves, I. S. *J. Lumin.* **2005**, *113*, 50–63.

(39) Fu, L.; Sá Ferreira, R. A.; Silva, N. J. O.; Fernandes, J. A.; Ribeiro-Claro, P.; Gonçalves, I. S.; de Zea Bermudez, V.; Carlos, L. D. *J. Mater. Chem.* **2005**, *15*, 3117–3125.

(40) Yu, X.; Su, Q. *J. Photochem. Photobiol., A: Chem.* **2003**, *155*, 73–78.

(41) Latva, M.; Takalo, H.; Mikkala, V. M.; Matachescu, C.; Rodriguez-Ubis, J. C.; Kanakare, J. *J. Lumin.* **1997**, *75*, 149–169.

(42) Steemers, F. J.; Verboom, W.; Reinhoudt, D. N.; Vander Tol, E. B.; Verhoeven, J. W. *J. Am. Chem. Soc.* **1995**, *117*, 9408–9414.

compared to other Eu^{3+} - β -diketonate complexes involving various nitrogen donors reported so far in the literature. Thus our results demonstrate that 3-phenyl-4-benzoyl-5-isoxazolone complexes of Eu^{3+} involving bidentate nitrogen may find potential application as emitting materials in organic light-emitting diodes.

Acknowledgment. The authors acknowledge financial support from the Defence Research and Development Organization and University Grants Commission, New Delhi,

India. The authors also thank Prof. T. K. Chandrashekar, Director Regional Research Laboratory, Trivandrum, India, and Prof. C. K. Jayasankar, S. V. University, Tirupathi, India, for their constant encouragement and valuable discussions.

Supporting Information Available: Crystallographic data, TG data, luminescence decay profiles, and phosphorescence spectra. This material is available free of charge via the Internet at <http://pubs.acs.org>.

IC061425A